CHAPTER II

THEORY

2.1 Zeolites

Zeolites are ordered, porous, and rigid crystalline aluminosilicates having a definite structure with a framework based on an extensive three-dimensional network of SiO_4 and AlO_4 tetrahedral. The tetrahedral are cross-linked by the sharing of oxygen atoms as shown in Figure 2.1

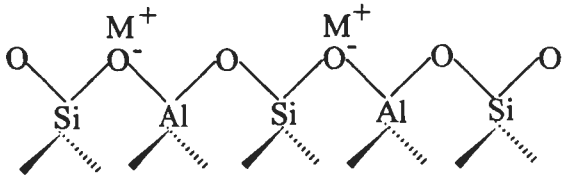

Figure 2.1 The structure of zeolites. [30]

The AlO_2^- tetrahedral in the structure determines the framework charge. This is balanced by cations that occupy nonframework positions. The general formula for the composition of zeolites is

$$M_{x/n}[(AlO_2)_x(SiO_2)_y].\ w\ H_2O$$

Where M is the cation of valence n, generally from the group I or II ions, although other metals, nonmetals, and organic cations are also possible, w is the number of water molecules. Water molecules presented are located in the channels and cavities, as the cations that neutralize the negative charge created by the presence of the AlO_2^- tetrahedral unit in the structure.

2.1.1 Zeolite Structures [30]

The structure of zeolite consisted of a three-dimension framework of the tetrahedral primary building units when tetrahedral atoms are silicon or aluminum as shown in Figure 2.2

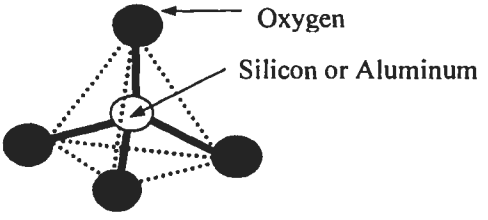

Figure 2.2 A primary building unit of zeolites.

Zeolites have a common subunit of structure so called primary building units of $(Al,Si)O_4$ tetrahedral, therein the Si or Al distribution is neglected. A secondary building unit (SBU) consists of selected geometric groupings of those tetrahedral. There are nine such building units, which can be used to describe all of the known zeolite structures. The secondary building units (SBU's) consist of 4,6 and 8-member single rings, 4-4, 6-6 and 8-8-member double rings, and 4-1,5-1 and 4-4-1 branched rings as illustrated in Figure 2.3

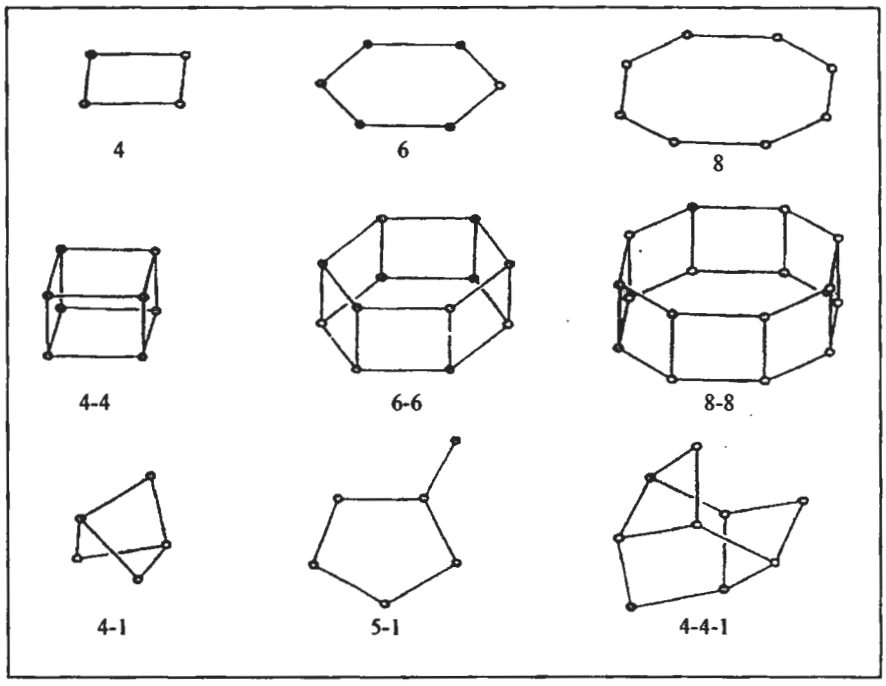

Figure 2.3 Secondary building units found in zeolite structures. [31]

Most zeolite frameworks can be generated from several different SBUs. For example, the sodalite framework can be build from either the single 6-member ring or the single 4-member ring. Some of them are shown in Figure 2.4

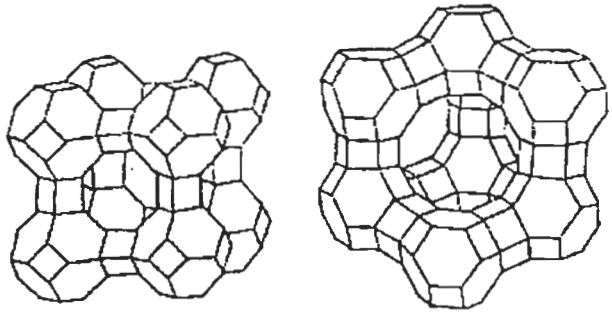

zeolite A faujasite

Figure 2.4 The structure of zeolite A and faujasite-type zeolites. [31]

2.1.2 Acid Sites of Zeolites

Most industrial application of zeolites are based upon technology adapted from the acid silica/alumina catalysts originally developed for the cracking reaction [20,23,26] .This means that the activity required is based upon the production of Brønsted acid sites arising from the creating 'hydroxyls' within the zeolites pore structure. These hydroxyls are formed by ammonium exchange followed by a calcination step. Zeolites as normally synthesized usually have Na^+ balancing the framework charges, but these can be readily exchanged for protons by direct reaction with an acid, giving hydroxyl groups, the Brønsted acid sites. Alternatively, if the zeolite is not stable in acid solution, it is common to use the ammonium, NH_4^+, salt, and then heat it so that ammonia is driven off, leaving a proton. Further heating removes water from Brønsted site, exposing a tricoordinated Al ion, which has electron-pair acceptor properties; this is identified as a Lewis acid site. A scheme for the formation of these sites is shown in Figure 2.5. The surfaces of zeolites can thus display either Brønsted or Lewis acid sites, or both, depending on how the zeolite is prepared. Brønsted sites are converted into Lewis sites as the temperature is increased above 500 °C, and water is driven off.

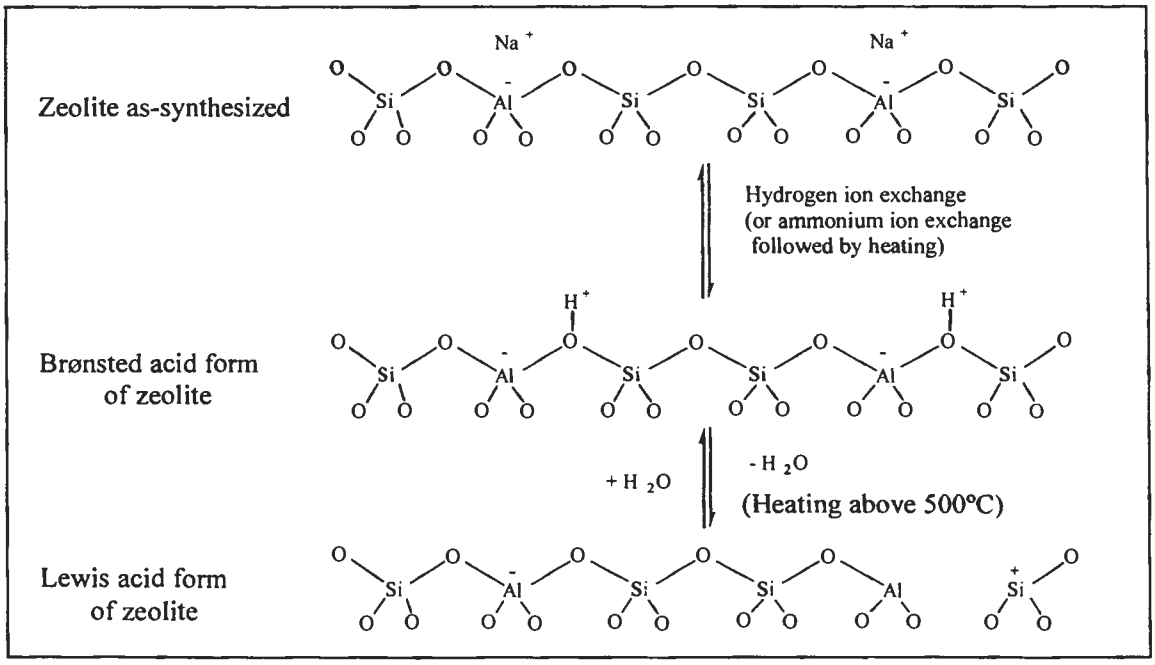

Figure 2.5 The generation of Brønsted and Lewis acid sites in zeolite. [32]

Hydrothermal syntheses of silica-rich zeolites generally consist of water as the solvent, a silicon source, an aluminum source, and a structure-directing agent. Better understanding of the effect of the structure-directing agent has long been aimed at. This will entail better control of the resulting structures, and even prediction of the specific structure could be possible. Some progress in the field has been made some general rules of correlation between the structure-directing agent and the structure of zeolites with high silica content:

1. Hydrothermal silicate syntheses result in dense crystalline and layered materials when no structure-directing agent is present.
2. Linear structure-directing agents usually result in one-dimensional molecular sieves with 10-ring channels.
3. Branched structure-directing agents tend to form multi-dimensional zeolites with pore diameters of 4-7 Å.
4. One-dimensional, large pore zeolites often result from large polycyclic structure-directing agents.

2.1.3 Shape Selectivity

Shape selectivity plays a very important role in catalysis. Highly crystalline and regular channel structures are among the principal features that zeolite used as catalysts offer over other materials. Shape selectivity is divided into 3 types: reactant shape selectivity, product shape selectivity and transition-state shape selectivity. These types of selectivities are shown in Figure 2.6. Reactant shape selectivity results from the limited diffusivity of some reactants, which cannot effectively enter and diffuse inside the zeolites. Product shape selectivity occurs when diffusing product molecules cannot rapidly escape from the crystal, and undergo secondary reactions. Restricted transition-state shape selectivity is a kinetic effect arising from the local environment around the active site: the rate constant for a certain reaction mechanism is reduced if the necessary transition state is too bulky to form readily.

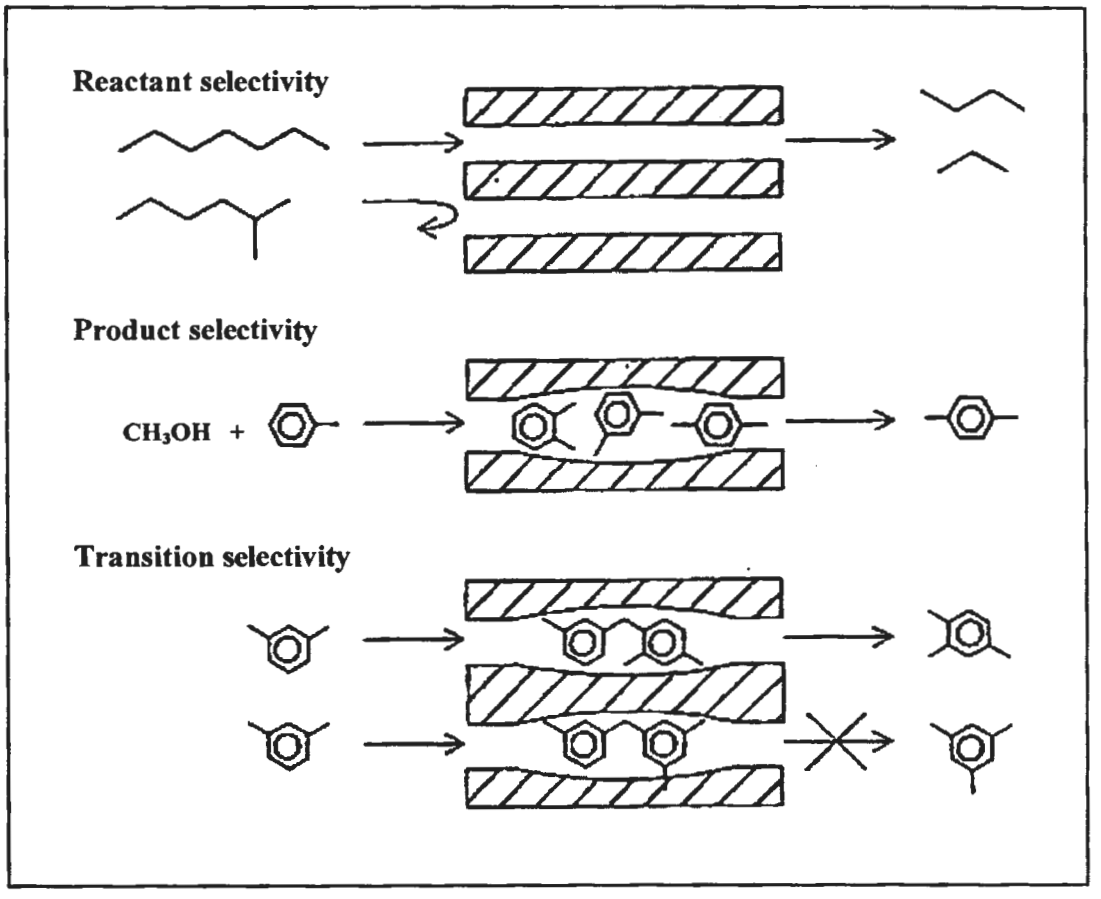

Figure 2.6 Three types of selectivity in zeolites: reactant, product and transition-state shape selectivity. [33]

2.2 Mesoporous Materials

Two classes of materials that are extensively as heterogeneous catalyst and adsorption media are microporous and mesoporous materials. Well-known members of the microporous class are zeolites, which provide excellent catalytic properties by the virtue of their crystalline aluminosilicate framework. However, their applications are limited by the relatively small pore openings. Many attempts to synthesize zeolites with larger pores have been made, but they were unsuccessful. Larger pores are present in porous glasses and porous gels, which were known as mesoporous materials.

In 1992, researchers at Mobil Corporation discovered the M41S family of silicate/aluminosilicate mesoporous molecular sieves with exceptionally large uniform pore structures, which has resulted in a worldwide resurgence in this area. The template agent used is no longer a single, solvated organic molecule or metal ion, but rather a self-assembled surfactant molecular array as suggested initially. Three different mesophases in this family have been identified, i.e., lamellar, hexagonal, and cubic phase. MCM-41 [34] has a hexagonally packed array of cylindrical pores. The structure of MCM-48 [35] has a three-dimensional, cubic-ordered pore structure and MCM-50 [36] contains a lamellar structure as illustrated in Figure 2.7

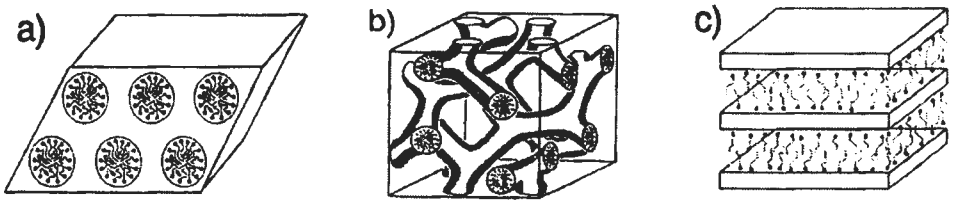

Figure 2.7 A schematic presentation of three inorganic-surfactant mesostructures: (a) the hexagonal phase, (b) the cubic phase, and (c) the lamellar phase.

Recently there are many families of mesoporous materials. Especially, new mesoporous member with hexagonal structure was discovered, such as HMS (Hexagonal Mesoporous Silica) [37], FSM-16 (Folded Sheets Mesoporous Materials) [38] and SBA-15 [39] with straight hexagonal structure. Because different types of templates can be used for synthesizing hexagonal mesoporous materials at various pH of gel, the new hexagonal materials can be obtained. The interaction of various types of template with inorganic species for assembling these materials are different as summarized in Table 2.1, together with the condition typically employed for a synthesis.

Table 2.1 Various synthesis conditions of hexagonal mesoporous materials and the type of interaction between template and inorganic species.

Material	Template	Assembly	Media (pH)
MCM-41	Quaternary ammonium salt	Electrostatic	Basic or Acid
FSM-16	Quaternary ammonium salt	Electrostatic	Basic (pH = 8.5)
SBA-15	Amphiphilic triblock copolymer	Hydrogen bonding	Acid (pH = 1-2)
HMS	Primary amine	Hydrogen bonding	Neutral

MCM-41 and FSM-16 can be synthesized using quaternary ammonium salt as a template. In case of SBA-15, amphiphilic tribock copolymer can be modified as a template and must be synthesized in acid condition of hydrochloric acid. On the other hand, HMS can be prepared in neutral and environmentally benign condition using primary amine as a template. Although these materials have the same hexagonal structure, some properties are different as shown in Table 2.2.

Table 2.2 Properties of some hexagonal mesoporous materials [34,37,38,39]

Material	Pore size (Å)	Wall thickness (nm)	BET specific surface area (m^2/g)	Framework structure
MCM-41	15-100	1	>1000	Honey comb
FSM-16	15-32	-	680-1000	Folded sheet
SBA-15	46-300	3-6	630-1000	Rope-like
HMS	29-41	1-2	640-1000	Wormhole

2.2.1 MCM-41 [40]

MCM (Mobil Composition of Matter)-41, a member of the extensive family of mesoporous molecular sieves, displays an ordered structure with uniform mesopores arranged into a hexagonal, honeycomb-like lattice as shown in Figure 2.8.

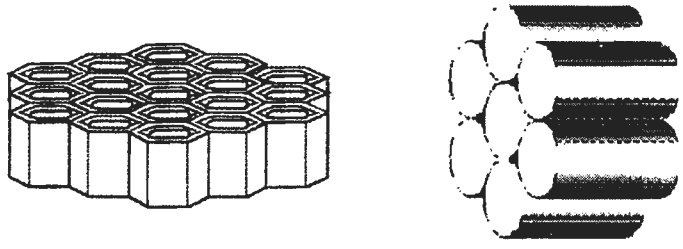

Figure 2.8 Hexagonal packing of unidimensional cylindrical pores.

MCM-41 has a very large specific surface area of approximately 1000 m^2/g. Reliable characterization of the porous hexagonal structure requires the use of five independent techniques:

(a) X-ray powder diffraction (XRD)

(b) Transmission electron microscopy (TEM)

(c) Nitrogen adsorption-desorption isotherm

(d) Temperature-programmed desorption (TPD) of ammonia

(e) Solid state ^{27}Al-MAS-NMR

2.2.1.1 Powder X-ray Diffraction (XRD) [41]

X-ray powder diffraction (XRD) is an instrumental technique used to identify minerals, as well as other crystalline materials. XRD is a technique in which a collimated beams of nearly monochromatic. X-rays is directed onto the flat surface of a relatively thin layer of finely ground material. XRD can provide additional information beyond basic identification. If the sample is a mixture, XRD data can be analyzed to determine the proportion of the different minerals present. Other information obtained can include the degree of crystallinity of the minerals present, possible deviations of the minerals from their ideal compositions, the structural state

of the minerals and the degree of hydration for minerals that contain water in their structure. Figure 2.9 shows a monochromatic beam of X-ray incident on the surface of crystal at an angleθ. The scattered intensity can be measured as a function of scattering angle 2θ. The resulting XRD pattern efficiently determines the different phases present in the sample.

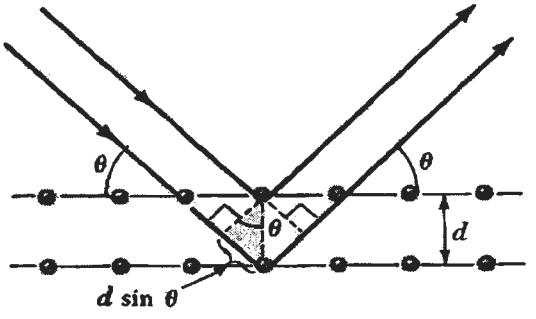

Figure 2.9 Diffraction of X-ray by regular planes of atoms. [42]

Using this method, Braggs' law is able to determine the interplanar spacing of the samples, from diffraction peak according to Bragg angle.

$$n\lambda = 2\,d\sin\theta$$

Where the integer *n* is the order of the diffracted beam, λ is the wavelength; *d* is the distance between adjacent planes of atoms (the *d*-spacings) and θ is the angle of between the incident beam and these planes.

2.2.1.2 Transmission Electron Microscopy (TEM) [43]

Transmission electron microscopy is an instrument which is ideally suited for the determination of the size and shape particles. Electron beam is transmitted through the specimen of small thickness. Since the intensity of the images depends on the sample thickness and concentration of atoms in the sample. To elucidate the pore structure of MCM-41, transmission electron microscopy is usually used. Figure 2.10 shows a TEM image of the hexagonal arrangement of uniform, 4 nm sized pores in a sample of MCM-41. The hexagonal morphology of MCM-41 can be easily observed in SEM as Figure 2.11 if the sample is conventionally prepared.

Figure 2.10 Transmission electron micrograph of MCM-41. [44]

Figure 2.11 Scanning electron micrograph of a MCM-41 sample. [45]

2.2.1.3 Nitrogen Adsorption-Desorption Isotherm

The N_2 adsorption technique is used to determine the physical properties of mesoporous molecular sieves, such as the surface area, pore volume, pore diameter and pore-size distribution of solid catalysts.

Adsorption of gas by a porous material is described by an adsorption isotherm, the amount of adsorbed gas by the material at a fixed temperature as a function of pressure. Porous materials are frequently characterized in terms of pore sizes derived from gas sorption data. IUPAC conventions have been proposed for classifying pore sizes and gas sorption isotherms that reflect the relationship between porosity and sorption. The IUPAC classification of adsorption isotherms is illustrated in

Figure 2.12. Six types of isotherms are characteristic of adsorbents that are microporous (type I), nonporous or macroporous (types II, III, and VI) or mesoporous (types IV and V).

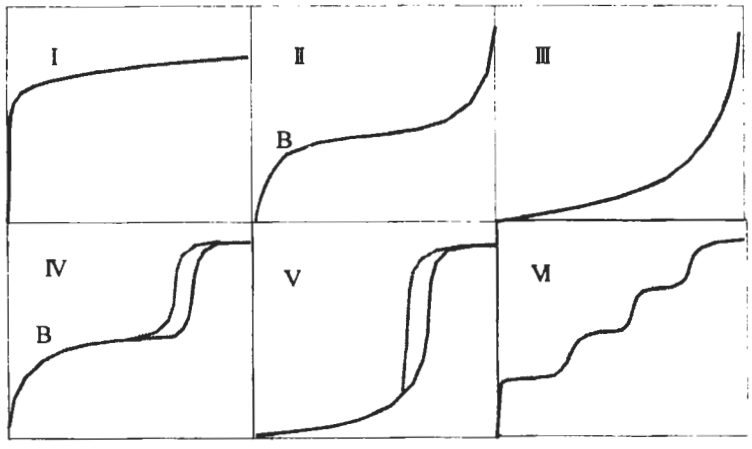

Figure 2.12 The IUPAC classification of adsorption isotherm. [46]

Adsorption isotherms are described as shown in Table 2.3 based on the strength of the interaction between the sample surface and gas adsorbate, and the existence or absence of pores. Pore types are classified as shown in Table 2.4.

Table 2.3 Features of adsorption isotherms [47]

Type	Features	
	Interaction between sample surface and gas adsorbate	**Porosity**
I	Relatively strong	Micropores
II	Relatively strong	Nonporous
III	Weak	Nonporous
IV	Relatively strong	Mesopore
V	Weak	Micropores or Mesopore
VI	Relatively strong Sample surface has an even distribution of energy	Nonporous

Table 2.4 IUPAC classification of pores [48]

Pore Type	Pore diameter / nm
Micropore	Up to 2
Mesopore	2 to 50
Macropore	50 to up

Pore size distribution is measured by the use of nitrogen adsorption/desorption isotherm at liquid nitrogen temperature and relative pressures (P/P_o) ranging from 0.05-0.1. The large uptake of nitrogen at low P/P_o indicates filling of the micropores (<20 Å) in the adsorbent. The linear portion of the curve represents multilayer adsorption of nitrogen on the surface of the sample, and the concave upward portion of the curve represents filling of mesopores and macropores.

The multipoint Brunauer, Emmett and Teller (BET) [49] method is commonly used to measure total surface area.

$$\frac{1}{W[(P_o/P)-1]} = \frac{1}{W_mC} + \frac{C-1}{W_mC}(P/P_o)$$

Where W is the weight of nitrogen adsorbed at a given P/P_o, and W_m is the weight of gas to give monolayer coverage, and C is a constant that is related to the heat of adsorption. A linear relationship between $1/W [(P_o/P)-1]$ and P/P_o is required to obtain the quantity of nitrogen adsorbed. This linear portion of the curve is restricted to a limited portion of the isotherm, generally between 0.05-0.30. The slope and intercept are used to determine the quantity of nitrogen adsorbed in the monolayer and calculate the surface area. For a single point method, the intercept is taken as zero or a small positive value, and the slope from the BET plot is used to calculate the surface area. The surface area reported depends upon the method used, as well as the partial pressures at which the data are collected.

2.2.1.4 Temperature-Programmed Desorption (TPD) of Ammonia [50]

Temperature-Programmed Desorption (TPD) is one of the most widely used and flexible techniques for characterizing the acid sites on oxide surfaces.

Determining the quantity and strength of the acid sites on alumina, amorphous silica-alumina, and zeolites is crucial to understanding and predicting the performance of a catalyst. For several significant commercial reactions (such as n-hexane cracking, xylene isomerization, propylene polymerization, methanol-to-olefins reaction, toluene disproportionation, and cumene cracking), all reaction rates increase linearly with Al content (acid sites) in H-ZSM-5. The activity depends on many factors, but the BrØnsted-acid site density is usually one of the most crucial parameters.

Preparation

Samples are degassed at 100 °C for one hour in flowing helium to remove water vapor and to avoid pore damage from steaming which may alter the structure of zeolites. The samples are then temperature programmed to 500 °C at a ramp rate of 10 °C/minute and held at that temperature for two hours to remove strongly bound species and activate the sample. Finally the sample is cooled to 120 °C in a stream of flowing helium.

Adsorption

Next the sample is saturated with the basic probe at 120°C; this temperature is used to minimize physisorption of the ammonia or organic amines. For ammonia, two techniques are available to saturate the sample: pulsing the ammonia using the loop or continuously flowing ammonia. Pulsing the ammonia allows the user to compare the quantity of ammonia adsorbed (via pulse adsorption) to the quantity desorbed for the subsequent TPD. After saturation with ammonia, pyridine, or propyl amine, the sample is purged for a minimum of one hour under a flow of helium to remove any of the physisorbed probes.

Desorption

The temperature-programmed desorption is easily performed by ramping the sample temperature at 10°C/minute to 500°C. It is a good rule of thumb that the end temperature during the TPD not exceed the maximum temperature used in the preparation of the sample.

Exceeding the maximum preparation temperature may liberate additional species from the solid unrelated to the probe molecule and cause spurious results.

During the TPD of ammonia or the non-reactive probes (pyridine or t-butyl amine), the built-in thermal conductivity detector (TCD) will monitor the concentration of the desorbed species. For the reactive probes (propyl amines), a mass spectrometer is required to quantify the density of acid sites. For these probes, several species may be desorbing simultaneously: amine, propylene, and ammonia.

2.2.1.5 ^{27}Al-MAS-NMR [51]

Another important characterization technique for mesoporous materials is solid state NMR. ^{27}Al-MAS-NMR spectroscopy has been employed to distinguish between tetrahedrally and octahedrally coordinated aluminum in the framework at approximately 50 and 0 ppm, respectively. Hence, the amount of framework aluminum can be determined.

2.3 Mechanism for Formation of MCM-41 Structure

2.3.1 Surfactant Templating

The synthesis mechanism for MCM-41 first proposed in 1992 by Beck *et al.*, [52,40] called "the liquid crystal templating mechanism", is shown in Figure 2.13 below. They suggest two different, possible synthesis pathways for the formation of the mesoporous structure, as visualized in Figure 2.13. In pathway 1, they suggest that the hexagonal, liquid-crystal surfactant phase exists in the solution before the silica precursors are added. The silica framework is precipitated around this template, forming a mesoporous structure. The surfactants are then removed by calcination, thus creating a porous structure with a high surface area. In pathway 2, they suggest that there is no ordered hexagonal structure in the solution before the silica is added. The silica precursors influence the surfactant aggregates, and the hexagonal structure is formed when the silica is added.

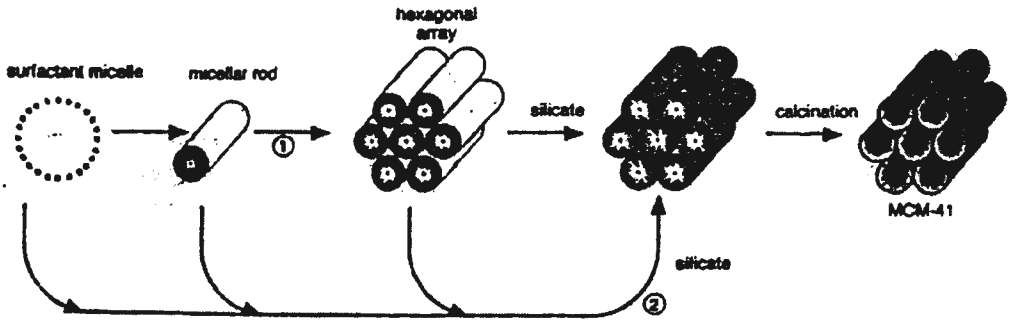

Figure 2.13 Possible synthesis pathways for the synthesis of MCM-41, by the liquid crystal templating mechanism. [52]

Chen *et al.* studied the synthesis mechanism of MCM-41 in more detail,[53] and they concluded that the formation of the mesostructure occurs by synthesis pathway number 2. They have investigated the formation mechanism by *in situ* ^{14}N-NMR and ^{29}Si-MAS-NMR, and proposed the mechanism as shown in Figure 2.14 below. In this model, the surfactants are aggregated as single, rod-like micelles before the addition of the silica precursors. When the silica is added, these species interact with the surface of the surfactant micelles, which cause the surfactant rods to assemble into a hexagonal array. Figure 2.14 also emphasizes the importance of gel aging during the hydrothermal treatment (step 4). During this step the silica is further condensed, and a more ordered and stable pore wall structure is obtained.

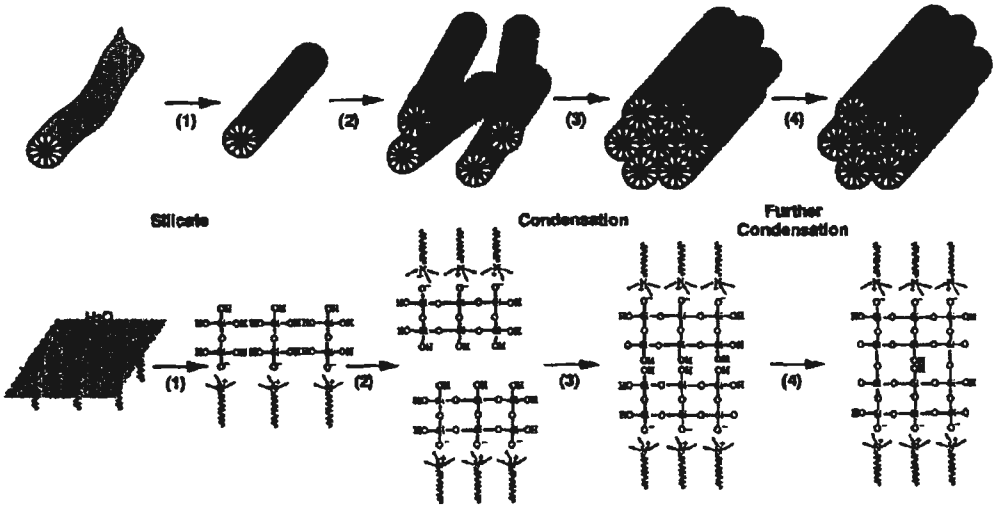

Figure 2.14 Proposed mechanism for the formation of MCM-41. [53]

2.3.2 Charge Density Matching

Stucky *et al.* made a major breakthrough in providing a general explanation for the synthesis mechanism for mesoporous materials, when they introduced the concept "charge density matching".[54,55] An illustration of the charge density matching process during formation of mesoporous materials is shown in Figure 2.15 below. Before the addition of the silica precursors, the surfactants are organized as single micellar aggregates of spherical or rod-like shape. Due to the alkaline conditions in the synthesis gel, the silica species are negatively charged. When the silica precursors are added to the surfactant solution, there is an electrostatic attraction between the anionic silica species and the surface of the cationic micelles. The silica species therefore polymerize at the micelle surface, thereby creating a negatively charged silica surface. Depending on the charge density of this silica surface, the surfactants then self-assemble into an ordered mesophase in order to match the oppositely charged silica surface. As the charge density of the surfactant mesophase is dependent upon the liquid-crystalline structure, the surfactants self-assemble into the structure that provides the best match to the silica surface (Figure 2.13). The obtained structure of the surfactant mesophase is therefore governed by the charge density matching process.

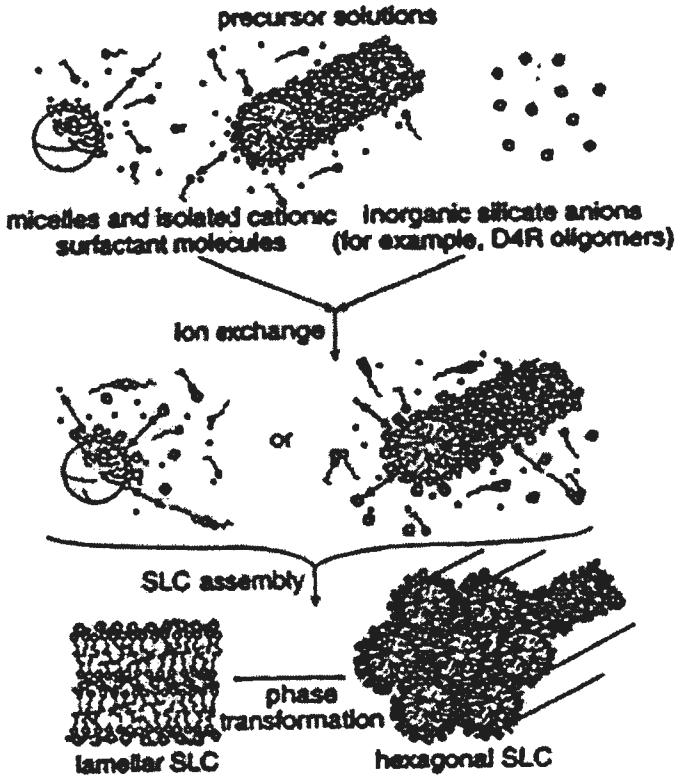

Figure 2.15 Illustration of the charge density matching process, as proposed by the group of Stucky. [54]

The formation of M41S materials shown in Figure 2.15 is an example of what has been called a (S^+I^-) synthesis mechanism, where the surfactants (S) are cationic and the inorganic precursors (I) are anionic. However, the charge density matching between these two phases may also occur through other possible synthesis routes such as (S^+I^+), if the surfactants are anionic and the inorganic species are cationic. Charge density matching between two equally charged surfaces may also occur, as in the ($S^+X^-I^+$) and ($S^-M^+I^-$) synthesis routes, where oppositely charged counterions function as charge balancing intermediates.

2.3.3 Folding Sheets [56]

Although the "folding sheets" mechanism, proposed by Inagaki *et al.*, is based on the intercalation of surfactant to layered silicates (kanemite) process, it should be elucidated here in order to give a comparison. Figure 2.16 is a schematic model representing the "folding sheets" mechanism. Initially, the surfactant cations

intercalate into the bilayers of kanemite via an ion exchange process. As the ion exchange proceeds, the interlayer cross-linking occurs by condensation of silanols. The silicate sheets of kenemite have the required flexibility to be folded due to its single sheet structure.

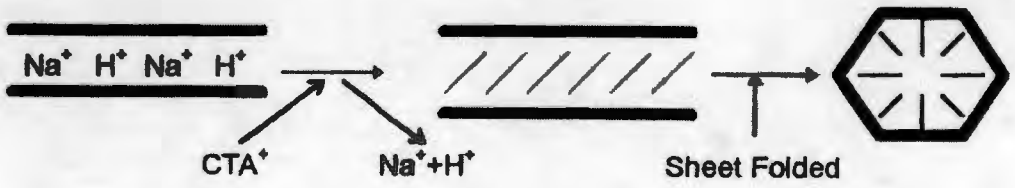

Figure 2.16 Model schematically representing "folding sheets" mechanism.

2.3.4 Silicate Layer Puckering

Instead of the formation of silicate-covered micellar rods, it was postulated that surfactant molecules assembled directly into the hexagonal LC phase upon addition of the silicate species, based on ^{14}N-NMR spectroscopy [57]. The silicates were organized into layers, with rows of the cylindrical rods intercalated between the layers as depicted in Figure 2.17. Aging the mixture caused the layers to pucker and collapse around the rods, which then transformed into the surfactant-containing MCM-41 hexagonal-phase mesostructure.

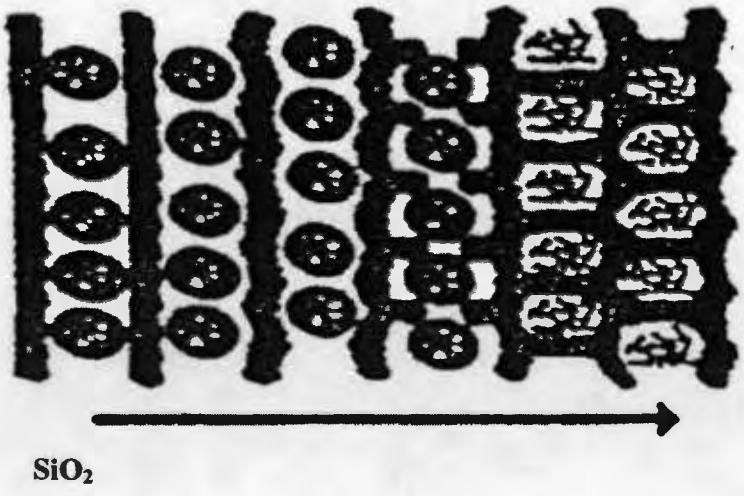

Figure 2.17 Puckering of silicate layers in the direction shown. [57]

2.3.5 Generalized Liquid Crystal Templating Mechanism Electrostatic Interaction

The formation mechanisms of the mesoporous silica in acid and alkaline conditions can be compared schematically in Figure 2.18.Using tetraethylorthosilicate (TEOS) as a silicon source, both mechanisms include a variety of phenomena: binding of the counterion and surfactant; the hydrolysis of TEOS; preferred polymerization of silicate species at the surfactant-silicate interface; and charged-matching combination of the surfactant and silicate oligomers. The primary distinction of the two formation process is in the cooperative interaction between surfactant and silica species. In alkaline condition, the silica species are negatively charged and thus energetically favored to condense at the surface of the positive charged surfactant (S^+) through the strong electrostatic interactions (S^+I^-). Thus the addition of counterion (X^-) with stronger binding affinity would decrease the number of active sites (S^+). In acid synthesis (pH<1), the dominating cationic silica precursor (I^+) combines with S^+X^- type active sites on the surfactant micelles through a weaker electrostatic interactions. To promote the silica condensation in $S^+X^-I^+$ without releasing X^-. Therefore, the counterion effect in the alkaline synthesis is opposite to the acidic synthesis.

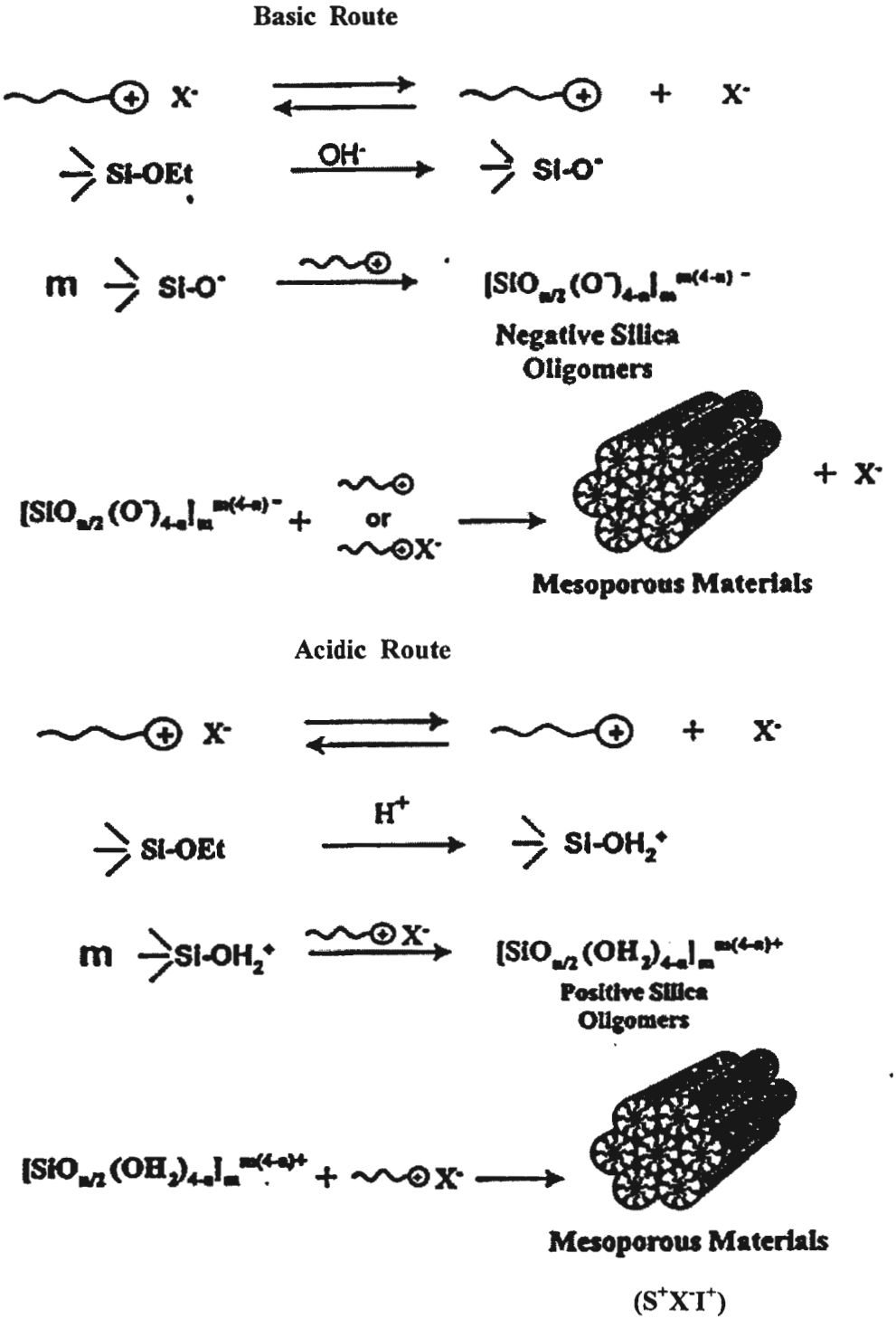

Figure 2.18 The comparison of the formation processes of the mesoporous materials in basic and acidic conditions. [58]

2.3.6 Effect of Parameters on the MCM-41 Synthesis

2.3.6.1 Effect of Surfactant

Vartuli *et al.* [59] have studied the effect of surfactant/silica molar ratio on the resultant phases in a simple system containing alkali metal, tetraethylorthosilicate (TEOS), water, and CTAOH at 100 °C. They found that as the surfactant/silica molar ratio increased from 0.5 to 2, the siliceous products obtained could be classified into three separate groups: MCM-41 (hexagonal), MCM-48 (cubic) and MCM-50 (lamellar). The data are in excellent agreement with the behavior of surfactants in solution as mentioned above [60].

The influence of alkyl chain length (C_6-C_{16}) and the reaction temperatures (100-200 °C) on the resulting products was also extensively investigated by Beck *et al.* [52] Figure 2.19 shows the XRD patterns of the products synthesized with different surfactants and at different temperatures. At 100 °C, with the increase of the surfactant alkyl chain length, the products are in the sequence of amorphous materials poorly defined MCM-41 well-defined MCM-41. At 150 °C, ZSM-5 zeolite with high crystallinity was generated from both the C_6 and C_8 surfactants. The C_{10} surfactant preparation produced less well-defined MCM-41 compared with the C_{12}, C_{14}, and C_{16} preparation. At 200 °C, ZSM-5 was synthesized from C_6; a mixture of ZSM-5, ZSM-48, and dense phases from $C_{8\text{-}14}$ surfactants; and amorphous phases from C_{16}. These data are also in good agreement with the surfactant solution chemistry [60,61]. Another interesting deduction from their study was that mesoporous and zeolite materials were not coproduced in the investigated temperature range using $C_{6\text{-}16}$ surfactants as templates. This behavior was explained in terms of the formation mechanism of MCM-41 which is quite distinct from that of the traditional zeolite templating mechanism.

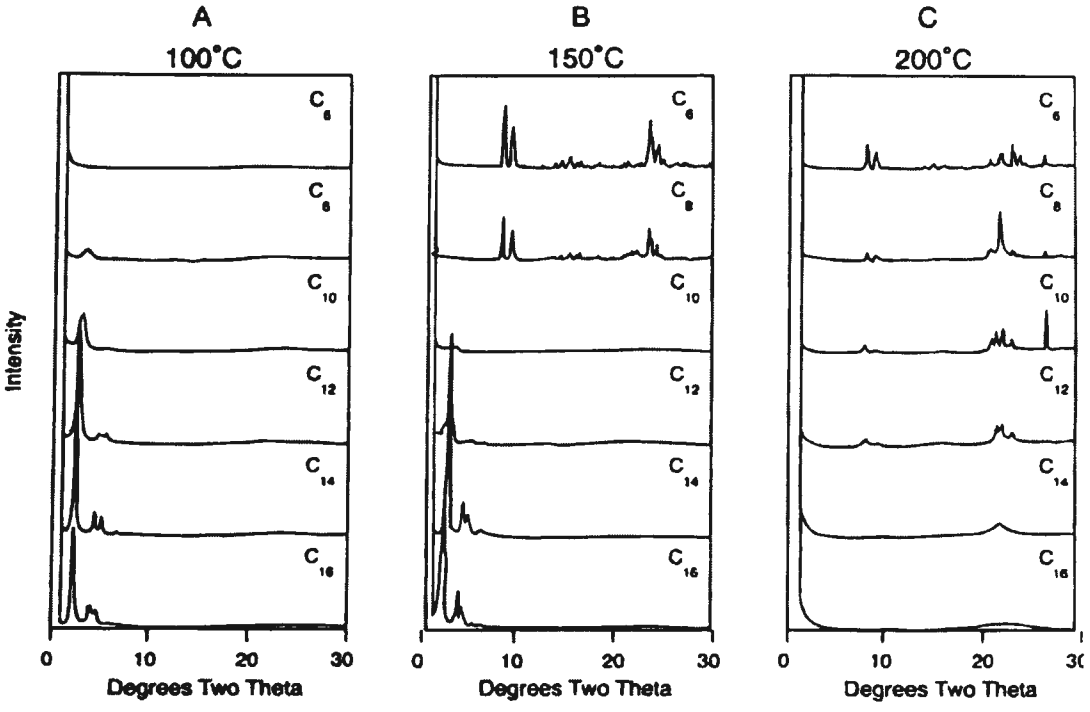

Figure 2.19 X-ray powder diffraction patterns of calcined products obtained using different surfactants at (A) 100, (B) 150, and (C) 200 °C [52].

2.3.6.2 Effect of pH Adjustment

The improvement of the structural and catalytic characteristics of MCM-41 type materials is of great importance in view of their applicability as catalysts and catalyst supports. A special post-synthesis treatment such as the extraction of the structure directing agent using acidic media prior to calcination has been shown to improve the thermal stability of Al-MCM-41. The variation of the synthesis parameters represents another possibility, since it was reported that the stability and characteristics of Al-MCM-41 are strongly affected by the synthesis conditions. The long-range order and stability of pure silica MCM-41 was improved through the intermediate pH adjustment of the synthesis gel [62,63]. Their results also suggested that this method could be extended to the synthesis of aluminum-containing MCM-41 [62]. Subsequent studies of the pH-adjustment synthesis of pure silica MCM-41 suggested a significant influence of the acid used for pH adjustment on the structure of the product and that the optimum pH for silica MCM-41 was 10. The earlier

investigations of Al-MCM-41 synthesis have shown that the pH adjustment improves the textural characteristics of these materials.

2.4 The Refining Process [64,65]

Every refinery begins with the separation of crude oil into different fractions by distillation (Figure 2.20). The fractions are further treated to convert them into mixtures of more useful saleable products by various methods such as cracking, reforming, alkylation, polymerization and isomerisation. These mixtures of new compounds are then separated using methods such as fractionation and solvent extraction. Impurities are removed by various methods, e.g. dehydration, desalting, sulphur removal and hydrotreating.

Refinery processes have developed in response to change market demands for certain products. With the advent of the internal combustion engine the main task of refineries became the production of petrol. The quantity of petrol available from distillation alone was insufficient to satisfy consumer demand. Refineries began to look for ways to produce more and better quality petrol. Two types of processes have been developed:

- Breaking down large, heavy hydrocarbon molecules
- Reshaping or rebuilding hydrocarbon molecules.

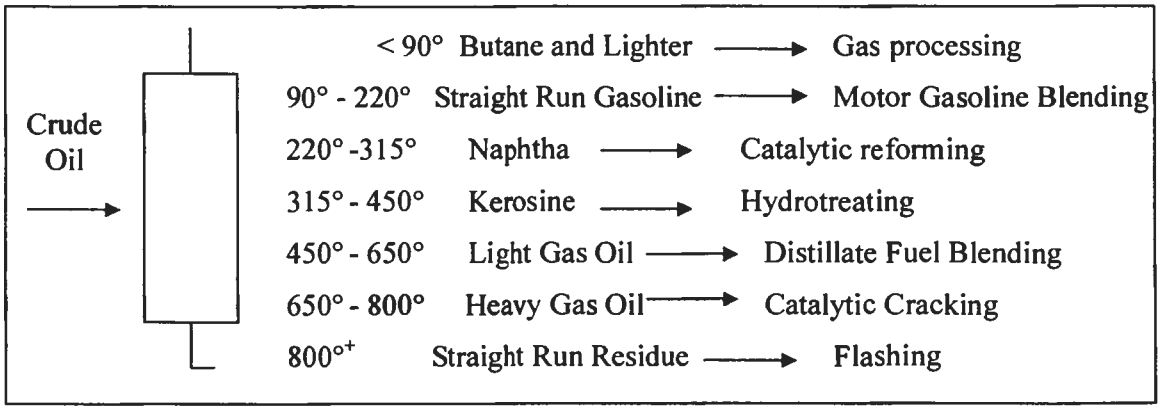

Figure 2.20 Distilling crude and product disposition.

Cracking processes break down heavier hydrocarbon molecules (high boiling point oils) into lighter products such as petrol and diesel. These processes include catalytic cracking, thermal cracking and hydrocracking.

- **Catalytic cracking** [66] is used to convert heavy hydrocarbon fractions obtained by vacuum distillation into a mixture of more useful products such as petrol and light fuel oil. In this process, the feedstock undergoes a chemical breakdown, under controlled heat (450°C-500°C) and pressure. Small pellets of silica-alumina have proved to be the most effective catalysts. The cracking reaction yield petrol, LPG, unsaturated olefin compounds, cracked gas oils, a liquid residue called cycle oil, light gasses and a solid coke residue. Cycle oil is recycled to cause further breakdown and the coke, which forms a layer on the catalyst, is removed by burning. The other products are passed through fractionators to be separated and separately processed.

- **Thermal cracking** [67]

In thermal cracking elevated temperatures (~800°C) and pressures (~700kPa) are used. An overall process of disproportionation can be observed, where "light", hydrogen-rich products are formed at the expense of heavier molecules which condense and are depleted of hydrogen. The actual reaction is known as homolytic fission and produces alkenes, which are the basis for the economically important production of polymers.

A large number of chemical reactions take place during steam cracking, most of them based on free radicals. Computer simulations aimed at modeling what takes place during steam cracking have included hundreds or even thousands of reactions in their models. The main reactions that take place include:

1. Initiation reactions, where a single molecule breaks apart into two free radicals. Only a small fraction of the feed molecules actually undergo initiation, but these reactions are necessary to produce the free radicals that drive the rest of the reactions. In steam cracking, initiation usually involves breaking a chemical bond between two carbon atoms, rather than the bond between a carbon and a hydrogen atom.

$$CH_3CH_3 \rightarrow 2\ CH_3\bullet$$

2. Hydrogen abstraction, where a free radical removes a hydrogen atom from another molecule, turning the second molecule into a free radical.

$$CH_3\bullet + CH_3CH_3 \rightarrow CH_4 + CH_3CH_2\bullet$$

3. Radical decomposition, where a free radical breaks apart into two molecules, one an alkene, the other a free radical. This is the process that results in the alkene products of steam cracking.

$$CH_3CH_2\bullet \rightarrow CH_2{=}CH_2 + H\bullet$$

4. Radical addition, the reverse of radical decomposition, in which a radical reacts with an alkene to form a single, larger free radical. These processes are involved in forming the aromatic products that result when heavier feedstocks are used.

$$CH_3CH_2\bullet + CH_2{=}CH_2 \rightarrow CH_3CH_2CH_2CH_2\bullet$$

5. Termination reactions, which happen when two free radicals react with each other to produce products that are not free radicals. Two common forms of termination are *recombination*, where the two radicals combine to form one larger molecule, and *disproportionation*, where one radical transfers a hydrogen atom to the other, giving an alkene and an alkane.

$$CH_3\bullet + CH_3CH_2\bullet \rightarrow CH_3CH_2CH_3$$

$$CH_3CH_2\bullet + CH_3CH_2\bullet \rightarrow CH_2{=}CH_2 + CH_3CH_3$$

- **Hydrocracking** can increase the yield of petrol components, as well as being used to produce light distillates. It produces no residues, only light oils. Hydrocracking is catalytic cracking in the presence of hydrogen. The extra hydrogen saturates, or hydrogenates the chemical bonds of the cracked hydrocarbons and creates isomers with the desired characteristics. Hydrocracking is also a treating process, because the hydrogen combines with contaminates such as sulphur and nitrogen, allowing them to be removed.

2.5 Catalytic Cracking Mechanisms

2.5.1. General Cracking Mechanisms [68]

In general, for components with equal carbon numbers, the rate of cracking decreases in the order: i-olefins > n-olefins > i-paraffins ≈ naphthenes > n-paraffins > aromatics. The cracking mechanism can be seen as a chain mechanism that involves the intermediate formation of carbocations, positively charged hydrocarbon species. Carbocations include both carbenium ions (e.g. $R_1{-}CH_2{-}C^+H{-}R_2$, $R_1{-}CH{=}C^+{-}R_2$)

and carbonium ions (e.g. $R_1–CH_2–C^+H_3–R_2$, $R_1–CH=C^+H_2–R_2$). In carbenium ions, the charge carrying carbon atom can be di- or tri-coordinated, while in carbonium ions, the charge carrying carbon atom is tetra- or pentacoordinated. The stability of the carbocations decreases in the order tertiary > secondary > primary [69]. Cracking of hydrocarbons is primary a reaction that proceeds through adsorbed carbenium ion intermediates.

2.5.2. Reactions of Olefins

The formation of carbenium ions from olefins can easily proceed by addition of the proton from a Brønsted acid site of the catalyst to the carbon–carbon double bond. Cracking of the adsorbed carbenium ion proceeds through the β-scission mechanism [70,71] or through the protonated cyclopropane mechanism [72]. An illustration is given in Fig. 2.21.

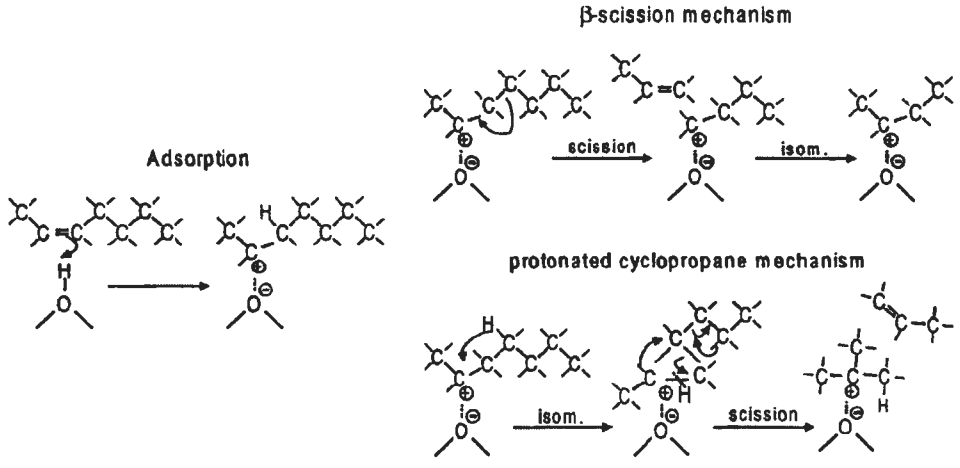

Figure 2.21 Cracking mechanisms illustrated by the reaction of n-heptene; adsorption at a Brønsted acid site leads to formation of an adsorbed carbenium ion that can be cracked. Both the β-scission mechanism [70,71] and the protonated cyclopropane mechanism [72] are shown.

Other reactions of the adsorbed carbenium ion are [73,74]:

1. Isomerization to a more stable carbenium ion, for example, through a methyl shift:

$$R_1–CH_2–C^+H–R_2 \rightarrow R_1–\underset{\displaystyle CH_3}{\overset{\displaystyle |}{C^+}}–R_2 + H^+ \qquad (1)$$

2. Oligomerization with olefin in a bimolecular reaction to form a larger adsorbed carbenium ion:

$$R_1\text{–}C^+H\text{–}R_2 + R_3\text{–}CH{=}R_4 \rightarrow R_1\text{–}\underset{\displaystyle R_3\text{–}CH_2\text{–}CH\text{–}R_4}{\overset{\displaystyle C^+\text{–}R_2}{\overset{|}{\underset{|}{}}}} \qquad (2)$$

3. Desorption with deprotonation to form an olefin (the opposite of adsorption):

$$R_1\text{–}CH_2\text{–}C^+H\text{–}R_2 \rightarrow R_1\text{–}CH{=}CH\text{–}R_2 + H^+ \qquad (3)$$

4. Desorption with hydride abstraction from a paraffin to form new paraffin from the carbenium ion and new carbenium ion from the paraffin (H-transfer reaction):

$$R_1\text{–}C^+H\text{–}R_2 + R_3\text{–}CH_2\text{–}R_4 \rightarrow R_1\text{–}CH_2\text{–}R_2 + R_3\text{–}C^+H\text{–}R_4 \qquad (4)$$

5. Desorption with hydride abstraction from (cyclic) olefins or coke (precursors) to form paraffin and a more aromatic compound (H-transfer reaction):

$$R_1\text{–}C^+H\text{–}R_2 + R_3\text{–}HC{=}CH\text{–}R_4 \rightarrow R_1\text{–}CH_2\text{–}R_2 + R_3\text{–}C^+{=}CH\text{–}R_4 \qquad (5)$$

The bimolecular reactions (2), (4) and (5) can occur if the pore size of the catalyst is large enough to accommodate the reactive intermediates, or they should occur on the outer surface of the zeolite particles. If the pores are too small, as in the case of ZSM-5 (0.53 nm× 0.56 nm), these reactions cannot take place with the larger (gasoline) components, although oligomerization or dimerization of small (C_2–C_4) olefins could be possible. For example, in the Mobil olefins to gasoline and distillates process (MOGD) coupling of light hydrocarbons is catalyzed by ZSM-5.

With ZSM-5, cracking through dimeric intermediates has only been reported in the reactions of relatively small *n*-olefins (C_4–C_6). Abbot and Wojciechowski [75] have studied cracking of *n*-olefins from C_5 to C_9 at 678K with ZSM-5 and found that cracking of pentene solely took place through a dimeric/disproportionation mechanism. Cracking of heptene and larger molecules proceeded mainly through monomolecular cracking and at 678 K; hexene represented the transition case of the two mechanisms and was cracked by both monomolecular cracking and through dimeric intermediates.

With Y-type zeolites, the dimeric mechanism is a more important reaction route; for example, it has been found that cracking of C_7 took place for 25% via a dimeric disproportionation reaction at 746K and for 32% at 673K.

2.5.3. Proposed Cracking Mechanisms of Polymer [76]

For ZSM-5 the cracking reactions of larger C_7^+ olefins are restricted to simple β-scission reactions. The relatively straight chains (or parts of it) can enter the pores of ZSM-5, are adsorbed, split-off small olefins, and desorb. For example, the reaction of n-heptene over ZSM-5 (for simplicity only the β-scission mechanism) is shown in Fig.2.22. The adsorbed C_7-carbenium ion is cracked to propene and C_4-carbenium ion. Then C_4-carbenium isomerizes to butene or is cracked to two ethene molecules.

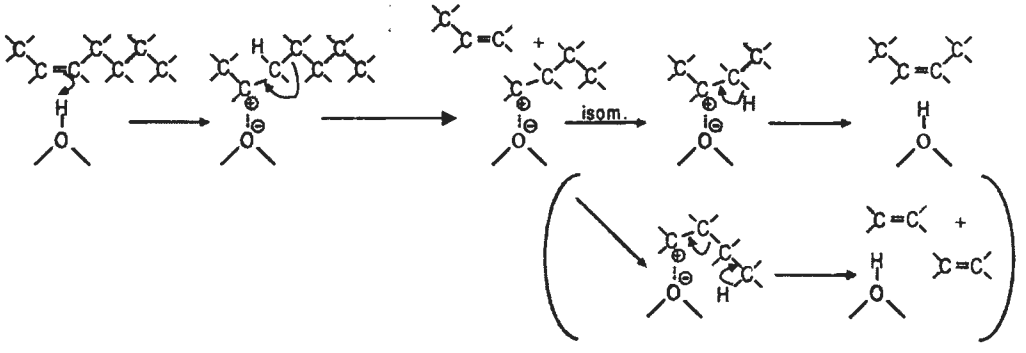

Figure 2.22 Monomolecular cracking mechanisms (only mechanism possible with ZSM-5).

Generally, the second reaction, formation of ethene, is energetically less favorable because it involves the formation of two primary carbenium ions. However, due to the small pores of ZSM-5, the electrical field in the pores is larger and a relatively large interaction between the catalyst and the adsorbed carbenium ions shall exist. It is believed that the oxygen atoms of a zeolite structure play a role in solvating carbocations, delocalizing the positive charge into the framework. The smaller the size of the pores of the zeolite, the closer the different oxygen atoms are to the adsorbed reaction intermediates and the higher the possible interaction. So possibly, as a result of increased stabilization of the intermediates, the formation of ethene is enhanced when small pore-zeolites such as ZSM-5 are involved.

On the base catalyst, with zeolite Y as active species (pore size 0.74 nm) adsorbed C_4-carbenium species and new heptene molecule to form an adsorbed C_{11}-carbenium ion. The C_{11} carbenium ion is cracked to hexane and C_5-carbenium ion. This bimolecular cracking mechanism proposed by Williams *et al.* [73] is illustrated in Fig. 2.23. Also, the adsorbed heptene carbenium ion could oligomerize before cracking.

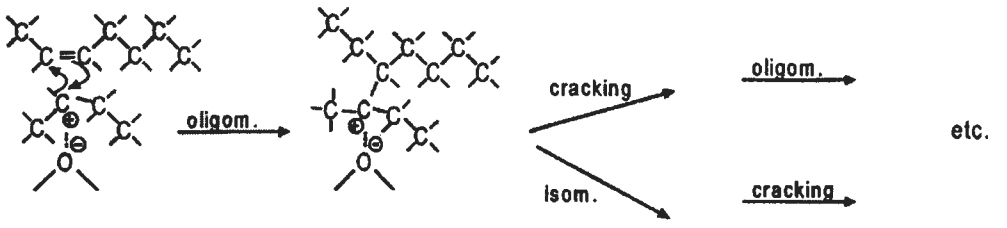

Figure 2.23 Bimolecular cracking mechanism that can occur on zeolite Y in addition to the monomolecular mechanism.

Because of the larger adsorption strength of larger hydrocarbons, the bimolecular mechanism have an important contribution in the cracking mechanism of the heavier gasoline-range olefins, provided that the catalyst pore size is large enough to accommodate the reaction intermediates. Aromatics and highly branched components, therefore, are too large to react through bimolecular mechanisms. Linear components are the most likely ones to react through this mechanism.

According to this proposed mechanism, the active site of ZSM-5 is the acid site itself, while the active site in zeoltie Y can be represented by the adsorbed carbenium ion. The reaction intermediates with ZSM-5 contain the number of carbon atoms (C_5–C_{11}), while the (surface) intermediates with the base catalyst can be much larger. As a result, the cracking products from ZSM-5 will be mainly C_3, C_4, and to some extent also C_2 olefins, while with the zeolite Y base catalyst larger fragments can be formed.

This agrees with the results that can be found in literature; the main products from *n*-olefins and *i*-olefins cracking on ZSM-5 are light olefins with a high selectivity for propene, *i*-butene, and in some cases the increased yields of ethene are reported.

A mechanism for the catalytic cracking of PE and PP using Al-MCM-41 as catalyst is proposed by Ishihara *et al.* [77,78]. As described, branched polyethylene components have short chains consisted of mainly of methyl groups.

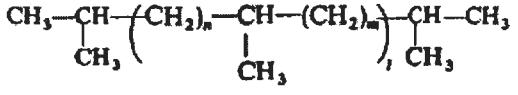

Where n+m=5, m=0-5
and l=2.3-6.7

Branching of the main fraction was at a frequency of one branch per three ethylene monomer units. The typical oligomer structure was found to be virtually the same as that of polyisoheptyl based on branching frequency. Moreover, oligomer chains showed random branching in an ethylene sequence in regular structures of polyisoheptyl. The catalytic cracking of PE is initiated by attack of low molecular weight carbonium ion (R^+) on a very small number of on-chain hydrogen atoms attached to tertiary carbon atoms in polymer chains. The initial reaction of molecular weight reduction is shown in equations (1). β-scission of on-chain carbonium ions (A) occurs to produce chain-ends (B) and (C):

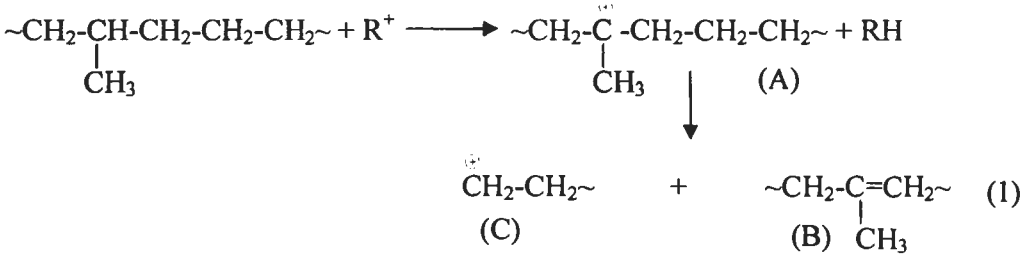

(1)

Mechanism of gas formation.

Gaseous products are produced from the liquid fraction produced by decomposition of oilgomers and reaction with typical oilgomers is shown in the following scheme. (where R^+ represents the volatile carbonium ion, $\sim CH_2\text{-}\overset{\overset{(+)}{|}}{C}H\text{-}CH_2$)

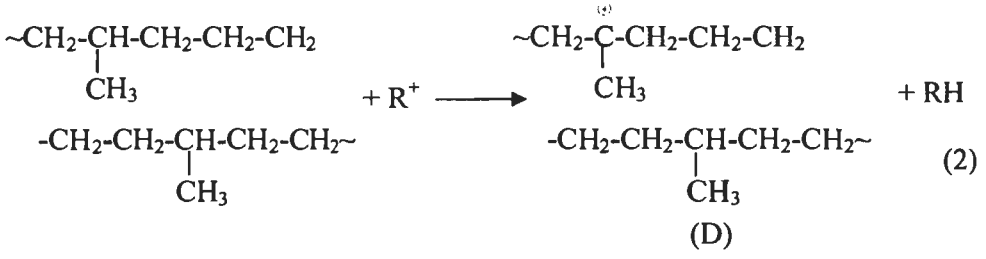

(2)

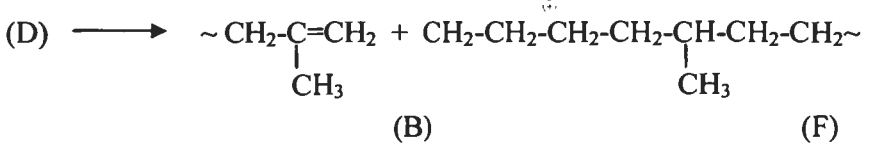

(3)

Gas formation takes place by way of the decomposition of these fractions. The unstable reaction intermediate (F) isomerized to secondary (G) or tertiary carbonium ions (H) as shown by equation (4).

From (F)

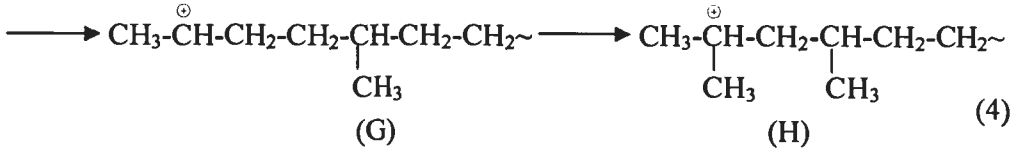

(4)

From (G)

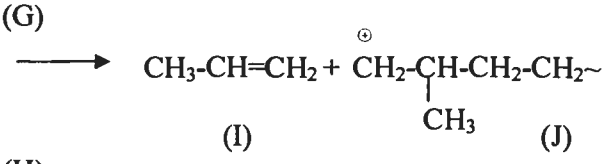

(5)

From (H)

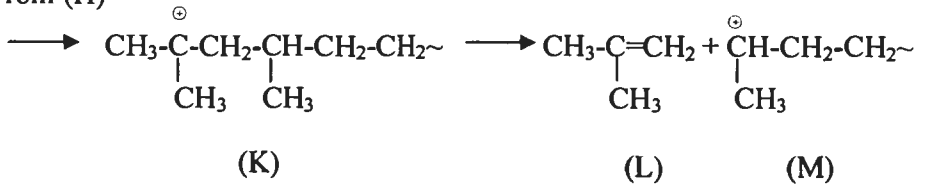

(6)

Ions (G) and (H) are essential to gaseous product formation and are mainly produced by β-scission of these carbonium ions (H). Isobutene is converted to isobutane through hydrogen transfer by the catalyst so that its yield is remarkably high. Propylene is produced in high yield by direct β-scission of other important ions (G) at high temperature.

The propane component is independent of propylene yield and is not produced by hydrogenation of propylene. The propane component is probably produced from propyl carbonium ions produced by β-scission of volatile tertiary carbonium ions without hydrogenation of propylene. For instance, stabilization of (F) ions takes place with lower activation energy of isomerization and thus intramolecular rearrangement to inner tertiary carbon atoms occurs. (F) ions cause intermolecular rearrangement by back biting reactions:

From (G)

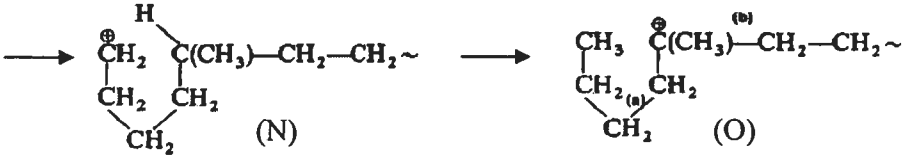

(7)

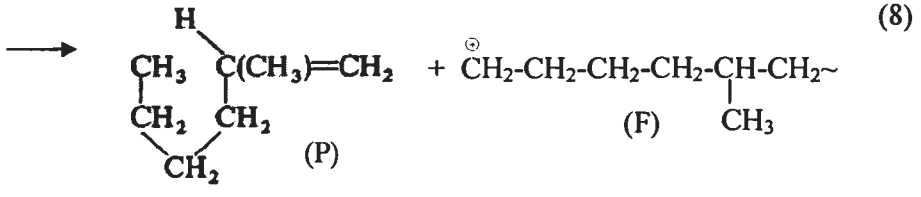

(8)

From (P)

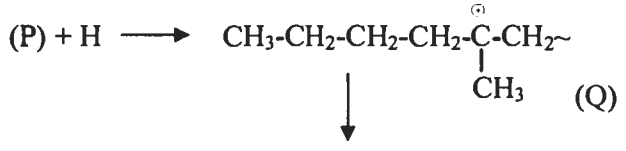

(9)

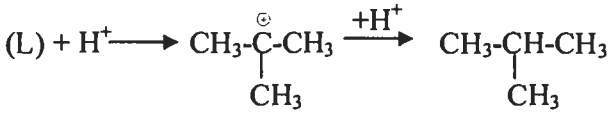

(10)

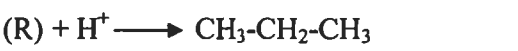

(11)

The stabilization of tertiary carbonium ions (O) proceeds by β-scission at the (b) position to give rise to a more stable fraction (P) than propyl ions ((a) position). Equations (7)-(11) show isobutene and propane are produced. Propane is not produced by the hydrogenation of propylene.

The mechanism of polypropylene is similar to polyethylene but the typical oligomer of polypropylene is 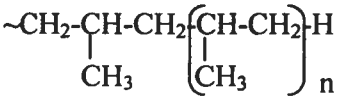

2.5.4. Reactions of Paraffins

Compared to olefins, paraffins have a lower reactivity towards cracking due to a more difficult formation of carbenium ions. Direct formation of a carbenium ion requires the abstraction of a hydride ion. This may proceed at Lewis acid sites or adsorbed carbenium ions can react with paraffins in a bimolecular-type of mechanism. The latter mechanism requires the presence of the adsorbed carbenium ions and can take place if the pore size of the catalyst is large enough to accommodate the necessary transition state (as is the case in zeolite Y and not in ZSM-5).

Indirect formation of carbenium ions is proposed to proceed through the formation of carbonium ions; paraffin reacts with a proton from a Brønsted acid site and the resulting adsorbed carbonium ion is cracked to an adsorbed carbenium ion and hydrogen or a small olefin. The formation of a carbonium ion requires an energetically unfavorable transition state and has high activation energy. This mechanism for activation of paraffins will only be significant in the absence of olefins

and is favored by high temperatures, low hydrocarbon partial pressures and low conversions of the paraffins. The occurrence is not expected to be significant when cracking a gasoline mixture that contains olefins. The olefin can easily form carbenium ions and cause cracking of paraffins through the bimolecular cracking mechanisms as discussed above.